South African Journal of Chemical Engineering 46 (2023) 394–403

Contents lists available at ScienceDirect

South African Journal of Chemical Engineering

journal homepage: www.elsevier.com/locate/sajce

Stability analysis of the shape factor effect of radiative on MHD couple stress hybrid nanofluid

Ali Rehman [a], Ma Chau Khun [a], Dolat Khan [b,*], Kamal Shah [c,d], Thabet Abdeljawad [c]

[a] Forensic Engineering Center Institute for Smart Infrastructure and Innovative Construction, Faculty of Civil Engineering, Universiti Teknologi Malaysia, Malaysia
[b] Faculty of Science, King Mongkut's University of Technology Thonburi (KMUTT), 126 Pracha Uthit Road, Bang Mod, Thung Khru, Bangkok 10140, Thailand
[c] Department of Mathematics and Sciences, Prince Sultan University, Riyadh 11586, Saudi Arabia
[d] Department of Mathematics, University of Malakand, Chakdara, Dir(L), KPK, Pakistan

ARTICLE INFO

Keywords:
Hybrid nanofluid
Stability analysis
Shrinking surface
Magneto hydrodynamics
Homotopy asymptotic method
Coupled equations

ABSTRACT

The insights of this study are implemented in a mathematical model with practical applications in industry, where they improve heat transport and minimize energy usage. The influence of the form factor on the radiative characteristics of a magnetohydrodynamic (MHD) pair stress hybrid nanofluid on a contracting surface is analyzed, along with the stability of the system as a whole. Enhancing the heat transfer ratio is the primary objective of this research because of its importance in the engineering and industrial fields. Nonlinear partial differential equations (PDEs) are formulated as a means of approaching the issue by taking into account the conservation principles of momentum and energy. Using a similarity transformation and thermophysical features, these PDEs are converted into ODEs. The resultant ODEs are solved using the approximate analytical approach known as Homotopy Analysis approach (HAM). The consequence of the relevant parameters, including couple stress parameter, magnetic field parameter, velocity ratio parameter, Prandtl number and Eckert number, on temperature distribution, Nusselt's number, velocity profile, and the skin friction are interrogated with the help of graphical representation. The velocity filed decreases with the increasing value of couple stress parameter, magnetic field parameter, and velocity ratio parameter. The temperature filed is increasing with the increasing value of Eckert number. The authors examine the convergence and stability of the problem using tables, graphs, and a dual solution strategy. In light of the significant difficulty encountered in heat transfer applications for cooling equipment and devices across a wide range of industries including automotive, microelectronics, defense, and manufacturing, this theoretical approach aims to positively contribute towards improving the heat transfer ratio to meet the demands of these sectors.

1. Introduction

The hunt for cutting-edge resources to recover energy and control heat transfer devices is now one of the most pressing topics being tackled by researchers. All forms of matter, including air and water, are included here. It is possible that the thermal efficiency of ordinary liquids might be improved by adding tiny solid metal particles to them. Suspended solid particles in fluids have been used in a number of methods to improve thermal efficiency by increasing heat transfer rates. Researchers' efforts in this area have received a lot of attention. Appreciatively, scientists have developed nanofluid, a unique fluid with unprecedented thermal efficiency and suspension stability. Scientists and engineers are interested in nanofluids because of the wide range of disciplines in which they may be used. Nanotechnology research has focused mostly on ways to improve heat transfer phenomena. The combination of liquid and solid components has been widely explored to increase heat transfer ratios in traditional fluids (Choi and Eastman, 1995 Oct 1). Choi and Eastman (1995 Oct 1) first introduced the term "nanofluid." Due to its importance in fields such as plasma research, hot rolling, nuclear reactors, wire drawing, and the fabrication of glass fibers, the flow of nanofluid across extensible surfaces in the presence of Lorentz effects has drawn substantial interest from researchers. Nanofluid boundary layer flow was studied by Makinde and Aziz (2011) using stretching surfaces. Rana and Bhargava (2012) looked at the flow and heat transfer of nanofluids by considering nonlinear stretching surfaces. Khan and Pop (2010) investigated nanofluid flow over a stretched sheet. By adding a nanofluid of changing viscosity, we were able to conduct

* Corresponding author.
E-mail address: dolat.ddk@gmail.com (D. Khan).

https://doi.org/10.1016/j.sajce.2023.09.004
Received 15 July 2023; Received in revised form 23 August 2023; Accepted 23 September 2023
Available online 25 September 2023

Nomenclature

U_w	Stretching/ Shrinking velocity (ms^{-1})
u and v	x and y components of velocity (ms^{-1})
T_w	Surface temperature
c	Coefficient of velocity for deformable plate
T_∞	Ambient temperature
ψ	Stream function
T_w	Wall temperature
η_0	Couple stress parameter
Re_x	Reynold number
ρ_{nf}	Nanofluid density
B_0	Magnetic field strength
σ	Electrical conductivity of the base fluid
$(\rho c_p)_{nf}$	Capacity of heat in Nano-fluid
N_t	Thermophore's parameter
hnf	Hybrid nanofluid
η	Similarity variable
ϕ	Volume fraction of nanoparticles
nf	Nanofluid
f	Base fluid
PDE's	Partial differential equations
HAM	Homotopy analysis method
τ	Time dependent parameter
x, y	Plane coordinate axis
C_{fx}	Coefficient of skin friction
a, b, c	Constants
β	Thermal expension coffecient
σ^*	Stefan-Boltzmann constant
Nu_x	Nusselt number
k^*	Mean absorption coefficient
α	Thermal diffusivity
μ	Dynamic viscosity
f'	Velocity without dimension
∞	Ambient condition
ν	Kinematic viscosity
θ	Temperature without dimension
Pr	Prandtl number
τ_w	Share stress of wall surface
p	Embedding parameter
q_w	Wall heat flux
SWCNT	Single wall carbon nanotube
ODE's	Ordinary differential equations
MWCNT	Multi wall carbon nanotube

MHD flow computations over a radiatively heated, radially expanding convective surface (Makinde et al., 2016). In order to study MHD nanofluids, Besthapu et al. (2017) used an expanding surface. Using a stretching surface, Acharya et al. (2016) investigated the impact of various measurements on MHD nanofluids. Acharya et al. (2016) studied Burger's nanofluid flow using two similar surfaces. Nanofluid behavior in the presence of an applied heat source was investigated by Das et al. (2016) using a contracting surface. To examine boundary layer flow, Ishfaq et al. (2016) used extending surfaces. Convective flow of nanofluids through heterogeneous porous surfaces was studied by Rana et al. (2012). Marangoni convection is significant in the field of fine skill equipment (Rehman et al., 2022), including ground paint applications. Pop et al. (2001) looked at many cases of Marangoni convection in thermo-solutal boundary films. Using a porous media, Al-Mudhaf and Chamkha (2005) studied Marangoni convection. Marangoni convection in thin film spray was investigated by Wang (1991) using a perturbation approach. The power law model was used by Chen (2007) to analyses Marangoni convection. High Reynolds numbers were utilised by Magyari and Chamkha (2007) to examine the impact of Marangoni convection. In Lin et al. (2013, 2014) investigated both the thermal gradients and the MHD Marangoni-convective. Laplace transform is utilised to explore Marangoni flow on a porous sheet in Aly and Ebaid (2016); Rehman et al. (2022). Ellahi et al. (2016) investigated several nano-scale material morphologies using an ethylene glycol base nanofluid. Permeable media were utilised by Jiao et al. (2016) to research Marangoni convection. MHD Marangoni convection and the concept of two phases nanoliquid hydrothermal were both researched by Sheikholeslami and Chamkha (2017). In addition to studying heat and mass transfer, they also look at hybrid nanofluid flow, which has significant uses in production of oil tanks, interruption bio engineering, atomic productions, polymer solutions, paper manufacture, geophysics, chemical manufacturing, and unusual oils, among other things (Eastman et al., 1996; Gul et al., 2020; Khan et al., 2022; Moldoveanu et al., 2019; Khan et al., 2023; Hameed et al., 2022; Wakif et al., 2021).

The extensive demand for thermal energy and the required heat transfer ratio for modern technologies cannot be met by commonly utilized fluids. When small atoms were added to base liquids to generate them, the base fluid's heat transfer ratio increased (Buongiorno et al., 2009). Thus, this increase in the thermal characteristics of common fluids stoked scientists' intense enthusiasm about conducting additional research. There exist lot of literature about carbon nanotubes and nanoparticles. Numerous researchers have produced CNTs with one or more walls (SWCNTs and MWCNTs). The carbon allotropes known as CNTs have a nano-cylindrical structure. They are substantially more dimensionally organised than the other nanoparticles. Used a lot in nanoscience and the energy sector (Kandasamy et al., 2016). Using an expanding surface, Rehman and Salleh (2021) studied the effect of a magnetic field on the time-dependent stagnation point flow of water-based GO-W and GO-EG. The flow of non-Newtonian Williamson fluids in thin films was studied by Ali et al. (2017), who used a stretched surface to do so. The flow of a viscous-dissipated hybrid nanoliquid exhibiting Darcy-Forchheimer phenomena was investigated by Gul et al. (2020) using a moving thin needle. Using water-based nanofluids, Mohyud-Din et al. (2015) investigated how velocity and temperature affected their flow. The nonlinear stretching cylinder was used by Abbas et al. (2023) to examine the radiative chemically reactive flow of induced MHD sutterby nanofluids. Using modified Fourier and Fick's equation, Shatanawi et al. (2023) studied heat and mass transfer in low-velocity fluid flow over a vertically sloping riga sheet. Nanomaterial micropolar fluid flow under exponential surface stretching was the primary research interest of Nadeem et al. (2020). Amjad et al. (2020), investigated who looked at the impact of Lorentz force and generated magnetic field effects. Javed et al. (2021) used sinusoidal wavy curved channel, investigate meta-analysis on homogeneous heterogeneous reaction effects. Nazir et al. (2021) used rotating heated porous cone, discus, hybrid nano-Carreau Yasuda fluid with hall and ion slip forces. Akbar and Sohail (2022) investigate 3D MHD viscous flow under the influence of thermal radiation and viscous dissipation. Sohail et al. (2021) used shooting method, investigate contribution of joule heating and viscous dissipation on 3D flow of Casson model. Wang et al. (2022) using non-Fourier's theory investigate tri-hybridized mixture in ethylene glycol comprising variable diffusion and thermal conductivity. Algehyne et al. (2022) using finite element approach study the thermal performance of Maxwell hybrid nanofluid boundary value problem. Sohail et al. (2020) used numerical approach, investigate entropy for the variable thermophysical characteristics of couple stress material. Sohail et al. (2020) study computational exploration for radiative flow of Sutterby nanofluid with variable temperature-dependent thermal

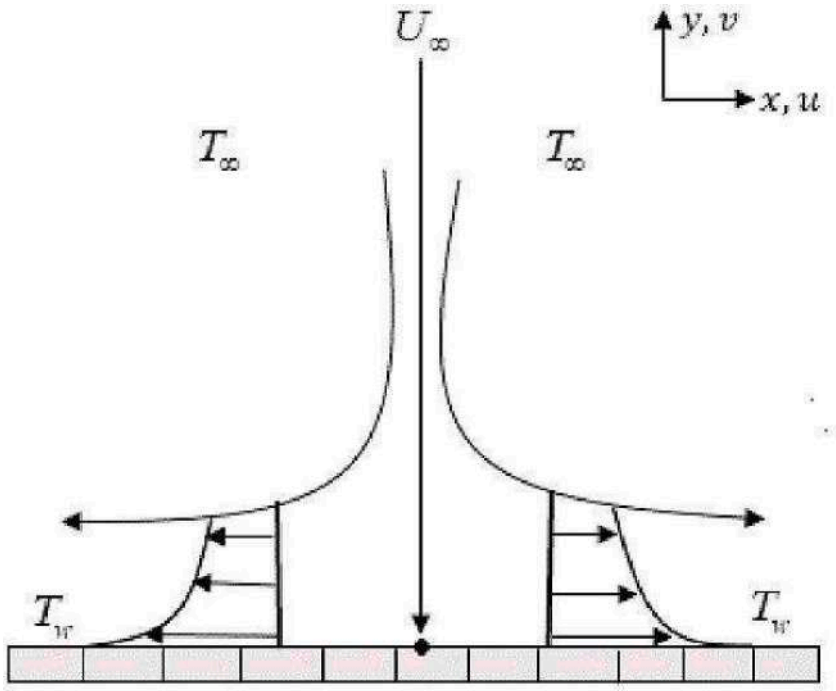

Fig. 1. Geometry as per problem formulation.

conductivity. Naseem et al., (2021) study contribution of dufour and soret effects on hydromagnetized material comprising temperature-dependent thermal conductivity. Nazir et al. (2022) study variable thermal properties in Carreau material with ion slip and Hall forces towards cone. Zubair et al. (2021) investigate Computational analysis of radiative Williamson hybrid nanofluid comprising variable thermal conductivity. Rizk et al. (2022) investigate the Influence of the KKL correlation model on the activation of thermal energy for the hybrid nanofluid flow over porous vertically rotating sheet. Abbas et al. (2023) investigate comparative analysis of time dependent flow of induced MHD radiative sutterby fluid flow at nonlinear extending surface. Abbas et al. (2023) investigate transportation of nanomaterial Maxwell fluid flow with thermal slip under the effect of Soret–Dufour and second-order slips. From the above stated in the previous literatures, the researchers give less attention to stability analysis of MHD couple stress hybrid nanofluid .Up to authors' knowledge, this model is not yet addressed analytically. This study aim to improve the heat transfer ratio by exploring the usage of hybrid nanofluid, which has been shown to be more effective at transferring heat than the base fluid. A unique element of this topic is discussed in detail, as the author provides an analytical discussion on the stability analysis of the form factor influence of Radiative on MHD pair stress hybrid nanofluid. The author does an approximate analytical analysis of the specified nonlinear DE. Data from the study is presented visually in the form of charts and tables. By computing the dual solutions, the authors also check the problem's convergence and stability. Specifically, the first observation of stability analysis on this model is highlighted, along with other novel parts of the newly released study, by the research results. In this study, the authors employ a contracting surface to conduct an analytical examination while the pair is under stress. The primary goals of this study are as follows:

1. Using a hybrid nanofluid to improve heat transfer efficiency.
2. Examining how well the approximation analytical approach converges.
3. Identifying which equations are stable and which are unstable, and why.
4. Examining how different variables affect velocity and temperature distributions.

1.1. Problem formulation

Time independent, two dimensional, laminar, incompressible, thermal flow of water based hybrid nanofluid $Te_2O_3 + MWCNTs + H_2O$ and nanofluid $SWCNTs + H_2O$, with velocity $U_w(x) = \frac{cx}{L}$, are considered over an Riga/EMHD, this plate deformed with (stretched and shrinking with linear velocity $U_w(x) = \frac{cx}{L}$, where c, is the coefficient of velocity for deformable plate, when c is positive represent stretching surface, when c, is negative then the surface is shrinking and when $c = 0$, than stand for EMHD plate, In this two-dimensional flow $x-$ axisis running along the sheet and y-axis is taken vertical to flow. The temperature at the surface is T_w, and the temperature away from the surface is T_∞, as shown in Fig. 1. The problem is modeled with help of following governing equations.

$$\frac{\partial u}{\partial x} + \frac{\partial v}{\partial y} = 0 \tag{1}$$

$$\left(u\frac{\partial u}{\partial x} + v\frac{\partial u}{\partial y}\right) = U_\infty \frac{dU_\infty}{dx} + \nu_{hnf}\frac{\partial^2 u}{\partial y^2} - \frac{\sigma_{hnf}}{\rho_{hnf}}{B_0}^2 u - \eta_0 \frac{\partial^4 u}{\partial y^4} \tag{2}$$

$$\left(\rho C_p\right)_{hnf}\left(u\frac{\partial T}{\partial x} + v\frac{\partial T}{\partial y}\right) = k_{hnf}\frac{\partial^2 T}{\partial x^2} + \frac{\partial q_r}{\partial y} + \mu_{nf}\left(\frac{\partial u}{\partial y}\right)^2, \tag{3}$$

The BCs are:

$$\begin{aligned} &u(0,\alpha t) = U_w(x), v(0,\alpha t) = 0, T(0,\alpha t) = T_w \ \text{ at } y = 0, \\ &u(0,\alpha t) = U_\infty, T(0,\alpha t) = T_w \ \text{ as } y = \infty \end{aligned} \tag{4}$$

$$q_r = -\frac{4\sigma^*}{3k^*}\frac{\partial T^4}{\partial y} \tag{5}$$

Using Eq. (5), in Eq. (3), we have

$$(\rho C_p)_{hnf}\left(u\frac{\partial T}{\partial x}+v\frac{\partial T}{\partial y}\right)=k_{hnf}\frac{\partial^2 T}{\partial x^2}-\frac{16\sigma^* T^3}{3k^*}+\mu_{nf}\left(\frac{\partial u}{\partial y}\right)^2, \tag{6}$$

Where ν_{hnf} is kinematic viscosity, σ_{hnf} electrical conductivity, ρ_{hnf} density of hybrid nano fluid repectively, B_0 is magnetic field strength, and η_0 is couple stress parameter, T represent the temperature, $\alpha$is thermal diffusivity of the base fluid, $T_w$and $T_\infty$are wall temperature and ambient fluid temperature respectively. To convert the fundamental flow Eqs. (1) – (5) from their dimensional to their dimensionless the following similarity transformation is applied

$$u=U_\infty(x)f'(\eta),\quad \eta=\left(\frac{U_\infty(x)}{x\nu_{hnf}}\right)^{\frac{1}{2}}y, v=-\left(\frac{U_\infty(x)\nu_{hnf}}{x}\right)^{\frac{1}{2}}f(\eta)\quad \text{and}\theta(\eta)=\frac{T-T_\infty}{T_w-T_\infty} \tag{7}$$

where η denote independent variable and ψ is stream function and defined as $u=\frac{\partial\psi}{\partial y}$ and $v=-\frac{\partial\psi}{\partial x}$, and is similarity variable. The following are the thermophysical properties of both nanofluid and hybrid nanofluid:

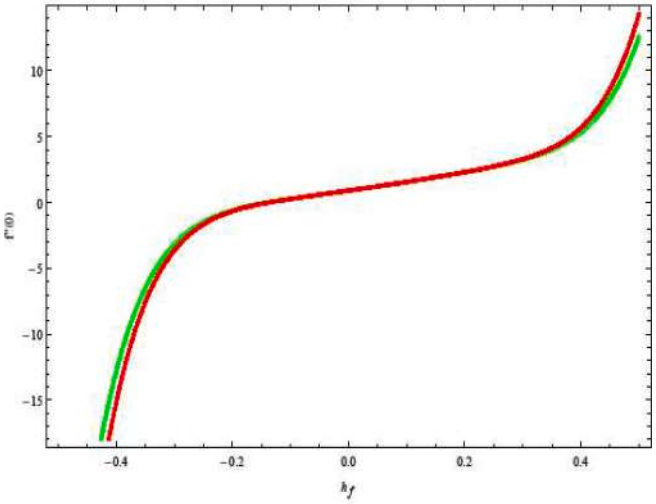

Fig. 2. h curve for velocity equation.

$$\left\{\begin{array}{l}\frac{\rho_{nf}}{\rho_f}=(1-\phi_1)+\frac{\rho_1\phi_1}{\rho_1},\quad \frac{(\rho C_p)_{nf}}{(\rho C_p)_f}=(1-\phi_1)+\rho_1\frac{(\rho C_p)_1}{(\rho C_p)_f},\quad \frac{(\rho\beta)_{nf}}{(\rho\beta)_f}=(1-\phi_1)+\rho_1\frac{(\rho\beta)_1}{(\rho\beta)_f}\\ \frac{\mu_{nf}}{\mu_f}=\frac{1}{(1-\phi_1)^{2.5}},\quad \frac{\sigma_{nf}}{\sigma_f}=1+\frac{3\left[\left(\frac{\sigma_1}{\sigma_f}-1\right)\phi_1\right]}{\left(\frac{\sigma_1}{\sigma_f}+2\right)\left(\frac{\sigma_1}{\sigma_f}-1\right)\phi_1},\quad \frac{k_{nf}}{k_f}=1+\frac{3\left[\left(\frac{k_1}{k_f}-1\right)\phi_1\right]}{\left(\frac{k_1}{k_f}+2\right)\left(\frac{k_1}{k_f}-1\right)\phi_1},\end{array}\right\} \tag{8}$$

$$\left\{\begin{array}{l}\frac{k_{nf}}{k_f}=\frac{\frac{k_1\phi_1+k_2\phi_2}{\phi_1+\phi_2}}{\frac{k_1\phi_1+k_2\phi_2}{\phi_1+\phi_2}}+\frac{2k_f+2(k_1\phi_1+k_2\phi_2)-2(\phi_1+\phi_2)k_f}{2k_f-2(k_1\phi_1+k_2\phi_2)+(\phi_1+\phi_2)k_f},\\ \frac{\mu_{hnf}}{\mu_f}=\frac{1}{(1-\phi_1-\phi_2)^{2.5}},\quad \frac{\rho_{hnf}}{\rho_f}=(1-\phi_2)\left[\left((1-\phi_2)+\phi_1\frac{\rho_1}{\rho_f}\right)\right]+\phi_2\frac{\rho_2}{\rho_f},\\ \frac{(\rho\beta)_{hnf}}{(\rho\beta)_f}=(1-\phi_2)\left[\left((1-\phi_2)+\phi_1\frac{(\rho\beta)_1}{(\rho\beta)_f}\right)\right]+\phi_2\frac{(\rho\beta)_2}{(\rho\beta)_f},\\ \frac{(\rho C_p)_{hnf}}{(\rho C_p)_f}=(1-\phi_2)\left[\left((1-\phi_2)+\phi_1\frac{(\rho C_p)_1}{(\rho C_p)_f}\right)\right]+\phi_2\frac{(\rho C_p)_2}{(\rho C_p)_f},\\ \frac{\sigma_{nf}}{\sigma_f}=1+\frac{3\left(\frac{\sigma_1\phi_1+\sigma_2\phi_2}{\sigma_f}\right)}{2+\left(\frac{\sigma_1\phi_1+\sigma_2\phi_2}{(\phi_1+\phi_2)\sigma_f}\right)}-\frac{3(\phi_1+\phi_2)}{\frac{\sigma_1\phi_1+\sigma_2\phi_2}{\sigma_f}-(\phi_1+\phi_2)}\end{array}\right\} \tag{9}$$

It is seen that the with the use of Eq (7) the continuity equation satisfied exactly, with use of Eq (7) and thermos-physical properties (8) and (9) in Eqs. (2) and (4) we get the following form of Eqs. (2) and (4):

$$\frac{(1-\phi_1-\phi_2)^{-2.5}}{(1-\phi_1-\phi_2)+\phi_1\left(\frac{\rho_1}{\rho_f}\right)+\phi_2\left(\frac{\rho_2}{\rho_f}\right)}f'''+ff''-M\mathrm{Re}(1-\phi_1)^{2.5}(1-\phi_2)^{2.5}f'^2+1-Kf^{iv}=0, \tag{10}$$

$$\frac{1}{\mathrm{Pr}}\frac{(1-\phi_1-\phi_2)^{-2.5}}{(1-\phi_1-\phi_2)+\phi_1\left(\frac{\rho_1}{\rho_f}\right)+\phi_2\left(\frac{\rho_2}{\rho_f}\right)}\frac{k_s}{k_{hnf}}\frac{4}{3}\theta'+(1-\phi_1)^{2.5}(1-\phi_2)^{2.5}f\theta'+Ec(f'')^2=0 \tag{11}$$

and the transform boundary conditions take the form

$$f'(0)=\lambda,\quad f(0)=0,\quad f(1)=0,\quad f'(0)=0,\quad \theta(0)=1,\quad f'(\eta)\to 0,\quad \theta(\eta)\to 0\quad \text{as}\quad \eta\to\infty, \tag{12}$$

where the following dimensionless parameters $M=\sigma_{hnf}B_0^2/\rho_{hnf}a$, $\mathrm{Pr}=\nu_{hnf}/\alpha$, $N_t=\tau D_T(T_w-T_\infty)/\nu_{hnf}T_\infty$, $\mathrm{Re}_x=\frac{u_w(x)x}{\nu_{hnf}}$, $K=\frac{\eta_0 a}{\nu^2_{hnf}\rho_{hnf}}$, $\phi_1=\frac{\nu_{nf1}}{\nu_{nf1}+\nu_{nf2}}$, and$\phi_2=\frac{\nu_{nf2}}{\nu_{nf1}+\nu_{nf2}++\nu_{nf3}}$, Magnetic field factor, Prandtl number, thermophore's factor, magnetic field parameter, Reynold number, couple-stress parameter, and nanoparticle volume fractions for nanofluid and hybrid nanofluid, respectively.

This is the dimensionless form and Nusselt number for skin friction:

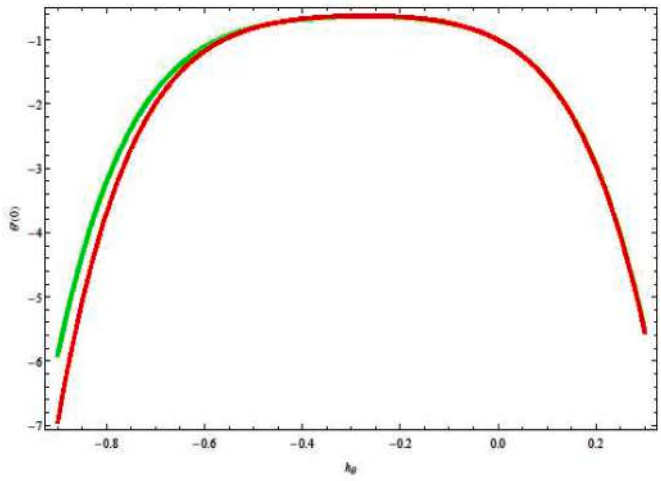

Fig. 3. h curve for temperature equation.

$$C_f = \frac{2\mu_{hnf}\left(\frac{\partial u}{\partial y}\right)_{y=0}}{\rho_{hnf}u_w^2}, \quad Nu = \frac{1}{k_f(T_w - T_\infty)}\left(k_{hnf}\frac{\partial T}{\partial y}\right)_{y=0}, \tag{13}$$

Applying Eqs. (7 – 9) in Eq. (13) which leads to

$$\sqrt{\mathrm{Re}_x}.C_f = \left(\frac{\sqrt{2}(1-\phi_1)^{2.5}.(1-\phi_2)^{-2.5}}{(1-\phi_2)\left\{\left((1-\phi_1)+\phi_1.\left(\frac{\rho_1}{\rho_f}\right)+\phi_2.\left(\frac{\rho_2}{\rho_f}\right)\right)\right\}}\right)f^{''}(0) \tag{14}$$

$$\frac{Nu}{\sqrt{\mathrm{Re}_x}} = -\frac{k_{hnf}}{k_f}\theta'(0) \tag{15}$$

2. Solution of problem

Skin friction causes a The homotopy asymptotic approach (HAM) (e. g., Liao (Shatanawi et al., 2023; Nadeem et al., 2020)) is used to acquire the analytical solutions of the given flow issue since it can be used to solve both linear and nonlinear problems. Good convergence of the described issue is achieved with the assistance of the BVP 2.0 software, which is used to minimize the total square residual error. The following are some approximate mensural forms and Nusselt numbers for velocity and temperature profiles:

$$f_0(\eta) = \frac{3}{2}\left[\frac{\eta^5}{5!} - \frac{\delta\eta^4}{2} + \left(\lambda - \frac{1}{2}\right)\eta + \left(\frac{1}{3} - \frac{\delta}{2}\right)\right].\left[\frac{-2(1+\lambda)^4}{(1+\lambda)^5}\right] \tag{16}$$

$$\theta_0(\eta) = 1.$$

The definitions of the linear operators for velocity $L_f$and $L_\theta$temperature are as follows:

$$L_f = \frac{d^5 f}{d\eta^5}\text{with}\left(C_1 + C_2\eta + C_3\eta^2\right)L_f = 0 \tag{17}$$

$$L_\theta = \frac{d^2\theta}{d\eta^2}\text{with}L_f\left(C_1 + C_2\eta + C_3\eta^2\right) = 0 \tag{18}$$

Velocity and temperature in Taylor's series expansion are given as:

$$f(\eta;\rho) = f_0(\eta) + \sum_{\xi=1}^{\infty} f_\xi(\eta)\rho^\xi, \tag{19}$$

$$\theta(\eta;\rho) = \theta_0(\eta) + \sum_{\xi=1}^{\infty} \theta_\xi(\eta)\rho^\xi. \tag{20}$$

2.1. Convergence analysis

Two series solutions, one for the velocity equation and one for the temperature equation, are found using HAM. The auxiliary functions h_f and h_θ, which help bring these two solutions closer together, are crucial to the convergence of the approach. Fig. 2 depicts the convergence of f ″(0), and Fig. 3 depicts the convergence of -curves at the 30th order of approximations.

3. Dual solution for stability analysis

Here the authors determine the stability of dual solutions under disturbances. Merkin (1986) first conducted this research, which was later expanded upon by Weidman et al. (2006). The time-dependent form of momentum and energy conservation is employed to produce the unstable stability, as in:

$$\rho_{hnf}\left(\frac{\partial u}{\partial t} + u\frac{\partial u}{\partial x} + v\frac{\partial u}{\partial y}\right) = U_\infty\frac{dU_\infty}{dx} + \nu_{hnf}\frac{\partial^2 u}{\partial y^2} - \sigma_{hnf}{B_0}^2 u - \eta_0\frac{\partial^4 u}{\partial y^4} \tag{21}$$

$$\left(\rho C_p\right)_{hnf}\left(\frac{\partial u}{\partial t} + u\frac{\partial T}{\partial x} + v\frac{\partial T}{\partial y}\right) = k_{hnf}\frac{\partial^2 T}{\partial x^2} + \frac{\partial q_r}{\partial y} + \mu_{nf}\left(\frac{\partial u}{\partial y}\right)^2, \tag{22}$$

and the BCs are

$$\begin{aligned} &u(0,\alpha t) = U_w(x), v(0,\alpha t) = 0, T(0,\alpha t) = T_w \ \text{ at } y = 0, \\ &u(\infty,\alpha t) = U_\infty, T(\infty,\alpha t) = T_w \ \text{ as } y = \infty, \end{aligned} \tag{23}$$

To obtain dimensionless form of Eqs. (21−23) we use the following transformation

$$\begin{aligned} &u = U_\infty(x)f^{'}(\eta), \quad \eta = \left(\frac{U_\infty(x)}{x\nu_{hnf}}\right)^{\frac{1}{2}}y, v = -\left(\frac{U_\infty(x)\nu_{hnf}}{x}\right)^{\frac{1}{2}}f(\eta) \\ &\text{and}\theta(\eta) = \frac{T - T_\infty}{T_w - T_\infty}, \text{and}\tau = at \end{aligned} \tag{24}$$

Using Eq. (24) in Eqs. (21 and 22) we get:

$$\begin{aligned} &\frac{(1-\phi_1-\phi_2)^{-2.5}}{(1-\phi_1-\phi_2)+\phi_1\left(\frac{\rho_1}{\rho_f}\right)+\phi_2\left(\frac{\rho_2}{\rho_f}\right)}\frac{\partial^3 f}{\partial\eta^3} + f\frac{\partial^2 f}{\partial\eta^2} - \\ &M\mathrm{Re}(1-\phi_1)^{2.5}(1-\phi_2)^{2.5}\left(\frac{\partial f}{\partial\eta}\right)^2 + 1 - K\frac{\partial^5 f}{\partial\eta^5} - \frac{\partial^2 f}{\partial\eta\partial\tau} = 0, \end{aligned} \tag{25}$$

$$\begin{aligned} &\frac{1}{\mathrm{Pr}}\frac{(1-\phi_1-\phi_2)^{-2.5}}{(1-\phi_1-\phi_2)+\phi_1\left(\frac{\rho_1}{\rho_f}\right)+\phi_2\left(\frac{\rho_2}{\rho_f}\right)}\frac{k_s}{k_{hnf}}\frac{4}{3}\frac{\partial^2\theta}{\partial\eta^2} + \\ &(1-\phi_1)^{2.5}(1-\phi_2)^{2.5}f\frac{\partial\theta}{\partial\eta} + Ec\left(\frac{\partial^2 f}{\partial\eta^2}\right)^2 - \frac{\partial\theta}{\partial\tau} = 0 \end{aligned} \tag{26}$$

Together with unsteady boundary conditions as given:

$$\begin{aligned} &f^{'}(0,\tau) = \lambda, \quad f(0,\tau) = 0, \\ &f(1,\tau) = 0, \quad f^{'}(0,\tau) = 0, \\ &\theta(0,\tau) = 1, \\ &f^{'}(\infty,\tau) = 0, \quad \theta(\infty,\tau) = 0 \end{aligned} \tag{27}$$

Now, take the following perturbation function as established

$$f(\eta,\tau) = f_0(\eta) + e^{-\gamma\tau}F(\eta), \qquad \theta(\eta,\tau) = \theta_0(\eta) + e^{-\gamma\tau}G(\eta). \tag{28}$$

Eq. (28) is apply a small disturbance $f = f_0(\eta)$ and $\theta = \theta_0(\eta)$ of Eq. (7) and (8). The function $F(\eta)$ and $G(\eta)$in Eq. (28), is comparatively less as compared to $f_0(\eta)$ and $\theta_0(\eta)$. The stability of the dual solution depend on the (positive or negative) value of the eigenvalue γ, now putting Eq. (27) in 26, (25) and (24) we have

Table 1
Thermo-physical properties of water, *CNTs* and Te_2O_3 nanoparticles.

	$\rho(kg/m^3)$	$C_p(j/kgK)$	$k(W/mK)$
Pure water	997.1	4179	0.613
SWCNTs	2600	425	6600
MWCNTs	1600	796	300
Te_2O_3	5200	670	6

Table 2
Residual errors versus number of iterations for velocity.

m	$f'(\eta)$
5	0.2211×10^{-2}
10	0.4204×10^{-3}
15	0.9101×10^{-5}
20	0.3531×10^{-6}
25	0.1270×10^{-7}

Table 3
Residual errors versus number of iterations for temperature.

m	$\theta(\eta)$
5	0.9390×10^{-1}
10	0.5120×10^{-2}
15	0.3218×10^{-3}
20	0.3651×10^{-4}
25	0.4483×10^{-5}

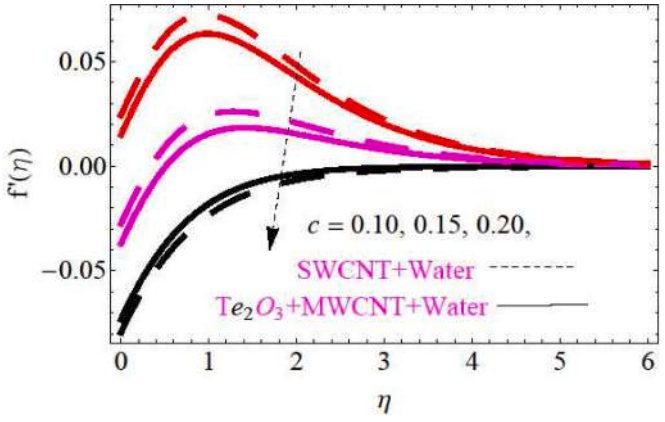

Fig. 4. Velocity profile via coefficient of velocity.

$$F''' + f_0 F'' - M\mathrm{Re}F'^2 + 1 - KF' + \gamma F^v = 0, \tag{29}$$

$$\frac{1}{\mathrm{Pr}}\frac{4}{3}G'' + f_0\theta' + Ec(F'')^2 - \gamma G = 0 \tag{30}$$

the BCs become

$$F'(0) = \lambda, \quad F(0) = 0, \quad F(1) = 0, \quad F''(0) = 0, \quad G(0) = 1, \quad F'(\infty) = 0, \quad G(\infty) = 0 \quad , \tag{31}$$

Setting $F''(0) = 1$, to obtained Eigenvalues of Eqs. (29) and (30).

Since the positive eigenvalue confirms the solution is stable and indicate the preliminary decline with passage of time and the negative eigenvalue shows the solution is unstable and indicates the preliminary growing of development with the passage of time.

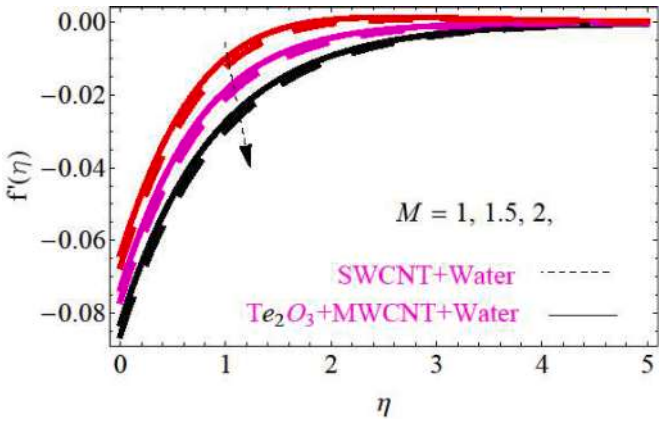

Fig. 5. Velocity profile via magnetic field parameter.

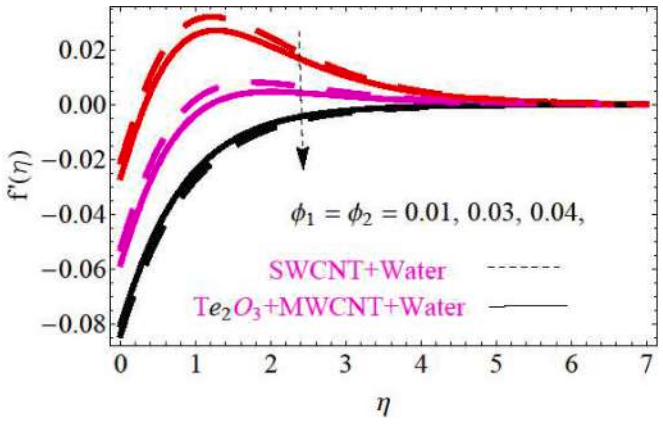

Fig. 6. Velocity profile via nanoparticle volume fraction.

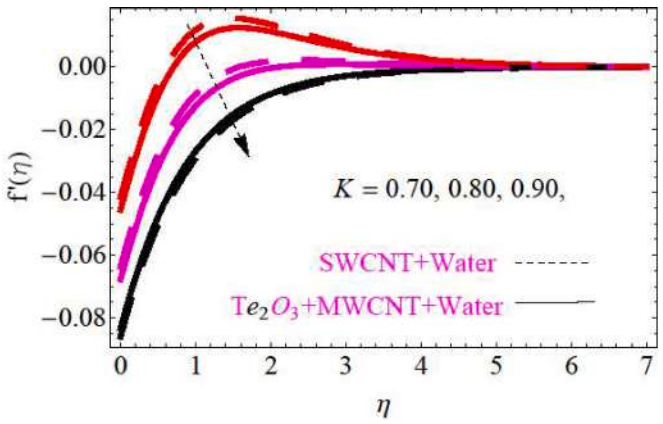

Fig. 7. Velocity profile via couple stress parameter.

3.1. Discussion and results follow

The objective of this work is to utilize water based hybrid nanofluid for thermal engineering applications that require rapid heating and cooling. Here a hybrid nanofluid having composition water as base liquid H_2O and, solid Te_2O_3, and *CNTs* as nanoparticles. The convergence of numerical solutions obtained from the implemented technique is fully investigated and confirmed. Thermo-physical characteristics of water and the properties of nanoparticles *CNTs*and Te_2O_3 reported in Table 1 are utilized in simulations. The residual errors versus the number of iterations for the velocity and temperature are reported in

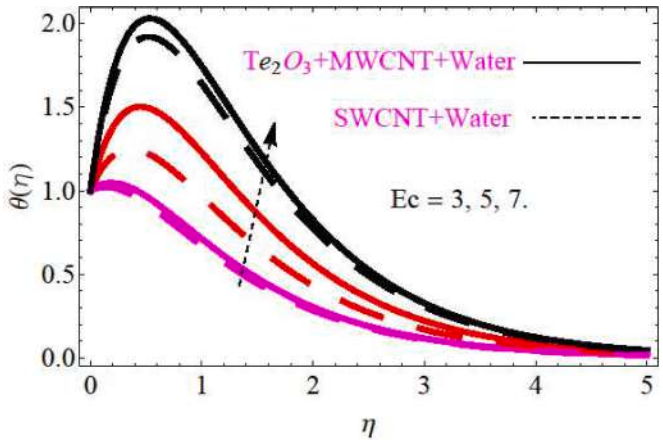

Fig. 8. Temperature profile via Eckert number.

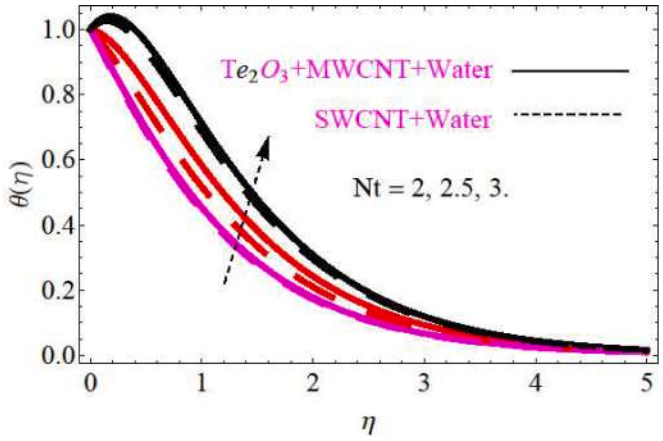

Fig. 9. Temperature profile via thermophore's parameter.

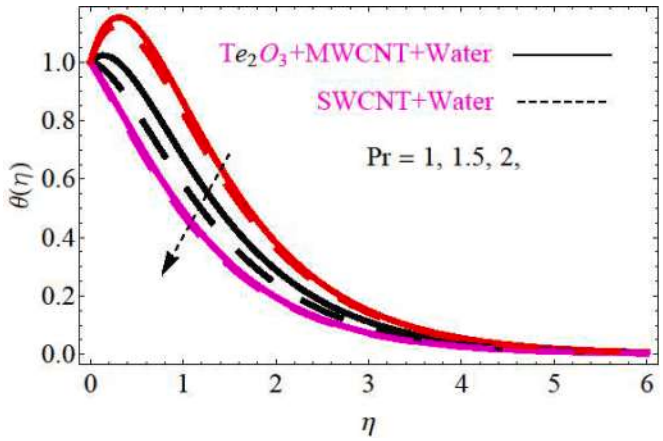

Fig. 10. Temperature profile via Prandtl number.

Tables 2 and 3, respectively. Clearly, the converged solutions are attained with increased number of iterations. Stability of the issue are shown in Table 6. To note the effects of involved parameters such as, magnetic-field parameter, nanoparticle volume fraction, couple-stress parameter, coefficient of velocity, thermophore's parameter, Prandtl number and Eckert number on graphical representations are given via these parameters for velocity profile and temperature distribution, skin friction, and Nusselt number as under: Fig. 2, shows h curve for velocity equation and Fig. 3, shows h curve for temperature equation.

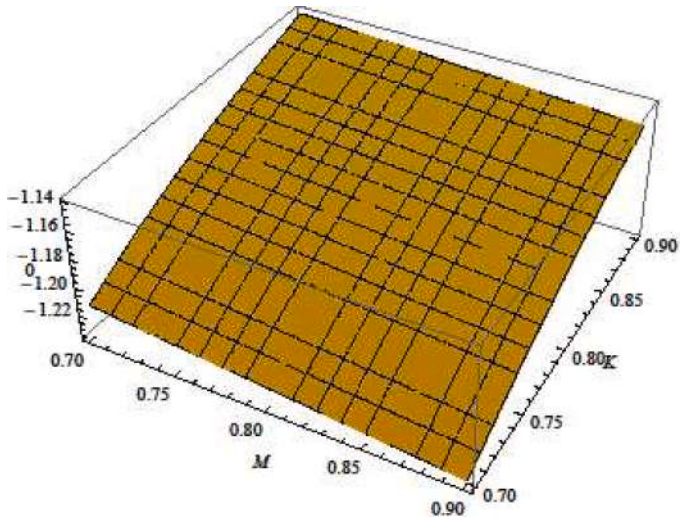

Fig. 11. Variation in skin friction due to couple stress parameter and magnetic field parameter.

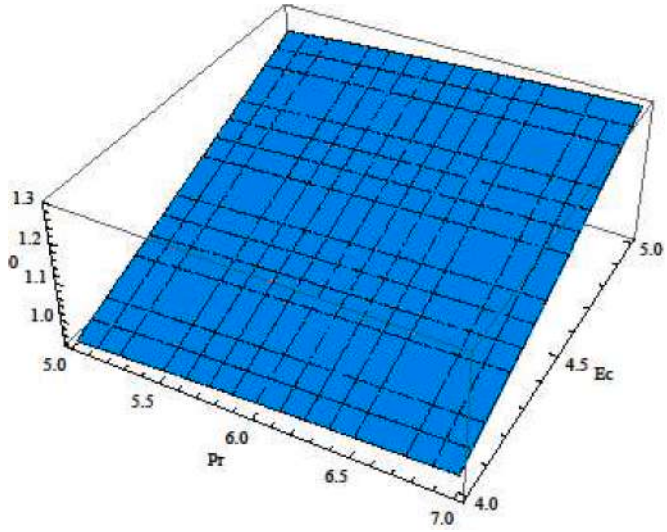

Fig. 12. Effect of fluid relaxation parameter and thermophore's parameter on Nusselt number.

Fig. 4 shows inverse correlation between the coefficient of velocity parameter and the velocity distribution of $Te_2O_3 + MWCNTs + H_2O$ and $SWCNTs + H_2O$, and found that increasing values of coefficient of velocity parameter decrease velocity profile of the fluids. Fig.5 is plotted to note the impact of magnetic field parameter on velocity profile $f'(\eta)$. It is observed that velocity is declines with the increasing values of the magnetic field parameter, shear thickening happens due magnetic field due to production of Lorentz forces. Fig.6 is sketched to note the effects of nanoparticle volume fraction $\phi_1 = \phi_2$ on velocity profile $f'(\eta)$. Increasing values of nanoparticle volume fraction increase the viscous forces inside the fluid due to which fluid velocity slow down and beneficial for heating purposes. Fig.7. is developed to note the impression of couple-stress parameter K, via velocity profile $f'(\eta)$. It is seen that the velocity profile and couple-stress parameter K have inverse relation. Increasing values of couple stress parameter rises the viscous forces due to which dropping behavior observed in the velocity profile and vice versa. Fig.8 is plotted to depicts the impact of Eckert number on temperature distribution $\theta(\eta)$ inside the fluids $Te_2O_3 + MWCNTs + H_2O$ and $SWCNTs + H_2O$. It is observed that both have directly proportional

Table 4
Influence of M, K, c, on the skin friction.

M	K	c	C_{fx}
1			0.7132
3			0.7451
5			0.7732
	0.70		0.7941
	0.80		0.8123
	0.90		0.8431
		0.10	0.8740
		0.50	0.9020
		0.90	0.9823

Table 5
Influence of Pr, Nt, Ec on Nusselt number.

M	Ec	N_t	Nu
1			1.5043
2			1.6035
3			1.7910
	7		1.8621
	8		1.9642
	9		2.0676
		1	2.1690
		1.5	2.2727
		2	2.5756

Table 6
Different smallest eigenvalue of γ when $c = 0.3, \quad K = 0.80 \text{and} M = 1.5,$.

M	γ 1st solution	2nd solution
1	0.1304	−0.1705
1.5	0.1501	−0.2204
2	0.2072	−0.2562
2.5	0.2204	−0.2768
3	0.2715	−0.3423
3.5	0.2901	−0.4312

relation, with the increasing values of Eckert number viscous forces have improving behavior due to which distribution of temperature improves. The effect of the thermophore's parameter Nt on the temperature profile is seen in Fig. 9. It has been observed that increasing the thermophores parameter values improves temperature distribution. The frictional force that is created in the fluid because of an increase in the thermophores parameter is what led to this improvement. This increment also helps in storing heat energy in $Te_2O_3 + MWCNTs + H_2O$, and $SWCNTs + H_2O$. Fig.10 shows the impact of Prandtl number Pr, on distribution of temprature $\theta(\eta)$. It is found that temprature distribution reduces due to increment in the amount of Pr. In this case viscous diffusion dominates thermal diffusion and in result temperature distribution slowdown in the fluid. The influence of the couple-stress parameter and the magnetic field on skin friction is seen in Fig. 11. Skin friction is observed to be negatively impacted by the couple-stress parameter and magnetic field. Skin friction gains strength because of the growth in surface friction forces caused by an increase in these parameters' values. Fig. 12 illustrates how the Nusselt number is affected by the thermophore's parameter and the Eckert number. These findings show that the thermophore's parameter and the fluid Eckert number both have an increasing effect on the Nusselt number. The increase in both forces heightens the Nusselt number in reward thermal energy stored in hybrid nanofluids due to increase in frictional and viscous forces. In addition to the graphical representation, The thermo-physical characteristics of nanoparticles and water are displayed in Table 1. Tables 2 and 3 display the residual errors for the velocity and temperature equations, respectively. Both tables indicate that as the number of iterations is increased, the residual errors decrease and there is substantial convergence. Table 4 also lists the influences of several parameters, such as M, K, c, on skin friction C_f. As can be observed, M, K, c, have a rising impact on skin friction; specifically, by increasing such parameters, the forces that create surface friction increase, which leads to an increase in skin friction. The impact of Pr, N_t, Ec, on the Nusselt number is given in Table 5. The collected results show that Pr, N_t, Ec, have an increasing relationship with the Nusselt number. The increasing values of Pr, N_t, Ec, help in the generation of frictional forces and in return hybrid nanofluid store the heat energy and Nusselt number improves. Table 6, shows the Stability analysis of dual solution of the issue .Since the dual solutions in this study are examined using a certain set of parameters, the major goal of stability analysis is to determine which of the solutions is more stable. The (boundary value problem) bvp4c solver in the Mathematica software is used to solve Eqs. (29 and 30) and boundary conditions (27), which assisted in providing analytical solutions to the equations. The composite values of M and the smallest eigenvalue γ are displayed in Table 6. Table 6 reveals that the first solutions display positive values whereas the second solutions exhibit negative values. The first solution is therefore stable, and the second one is unstable.

4. Conclusion

In this research, the authors analyze the stability of a hybrid nanofluid under the stress of a radiative-on-MHD pair. Improving the heat transfer ratio, an essential aspect of the engineering and industrial sectors, is the major focus of this investigation. After making sure the data is consistent, the issue is modeled according to the laws of momentum and energy conservation. Thermophysical features and a similarity transformation are used to convert modeled nonlinear PDEs to ODEs. The resulting ODEs are solved using HAM, and the influence of various parameters on the velocity profile and temperature distribution is shown via various graphical representations. The convergence and stability of the problem is presented in tables. The main conclusion of the current study can be summarized as follows:

i. Increasing values of via coefficient of velocity declines fluid velocity.
ii. Increasing values of magnetic field parameter, nanoparticle volume friction, couple stress parameter declines the fluid velocity.
iii. Increment in Eckert number and thermophore's parameter Nt enhances the distribution of temperature inside fluid.
iv. Fall in temperature distribution occurs due to reduction of thermal diffusion with rise in Prandtl number.
v. Increasing values of couple-stress parameter and the magnetic field strengthen skin friction of the fluid.
vi. Increment in the values of thermophore's parameter and the Eckert have positive impact on the Nusselt number and helps in heat energy storage.

Declaration of competing interest

The authors declare no conflict of interest.

Data availability

The data is available from the corresponding author on reasonable request.

Acknowledgements

Kamal Shah and Thabet Abdeljawad are thankful to Prince Sultan University for APC and support through the TAS research lab.
This study is funded Ali Rehman is a postdoctoral fellow of university

technology Malaysia under the postdoc fellowship scheme for the project; Q.J130000.21A2.07E1107E11.

References

Abbas, N., Shatanawi, W., Abodayeh, K., Shatnawi, T.A., 2023a. Comparative analysis of unsteady flow of induced MHD radiative Sutterby fluid flow at nonlinear stretching cylinder/sheet: variable thermal conductivity. Alex. Eng. J. 72, 451–461.

Abbas, N., Shatanawi, W., Shatnawi, T.A., 2023b. Transportation of nanomaterial Maxwell fluid flow with thermal slip under the effect of Soret–Dufour and second-order slips: nonlinear stretching. Sci. Rep. 13 (1), 2182.

Abbas, N., Shatanawi, W., Taqi, A.M., 2023c. Thermodynamic study of radiative chemically reactive flow of induced MHD sutterby nanofluid over a nonlinear stretching cylinder. Alex. Eng. J. 70, 179–189.

Acharya, N., Das, K., Kumar Kundu, P., 2016a. Ramification of variable thickness on MHD TiO 2 and Ag nanofluid flow over a slendering stretching sheet using NDM. Eur. Phys. J. Plus 131, 1–16.

Acharya, N., Das, K., Kundu, P.K., 2016b. The squeezing flow of Cu-water and Cu-kerosene nanofluids between two parallel plates. Alex. Eng. J. 55 (2), 1177–1186.

Akbar, S., Sohail, M., 2022. Three dimensional MHD viscous flow under the influence of thermal radiation and viscous dissipation. Int. J. Emerg. Multidiscip.: Math. 1 (3), 106–117.

Algehyne, E.A., El-Zahar, E.R., Elhag, S.H., Bayones, F.S., Nazir, U., Sohail, M., Kumam, P., 2022. Investigation of thermal performance of Maxwell hybrid nanofluid boundary value problem in vertical porous surface via finite element approach. Sci. Rep. 12 (1), 2335.

Ali, L., Islam, S., Gul, T., Khan, I., Dennis, L.C.C., Khan, W., Khan, A., 2017. The Brownian and thermophoretic analysis of the non-Newtonian Williamson fluid flow of thin film in a porous space over an unstable stretching surface. Appl. Sci. 7 (4), 404.

Al-Mudhaf, A., Chamkha, A.J., 2005. Similarity solutions for MHD thermosolutal Marangoni convection over a flat surface in the presence of heat generation or absorption effects. Heat Mass Transf. 42, 112–121.

Aly, E.H., Ebaid, A., 2016. Exact analysis for the effect of heat transfer on MHD and radiation Marangoni boundary layer nanofluid flow past a surface embedded in a porous medium. J. Mol. Liq. 215, 625–639.

Amjad, M., Zehra, I., Nadeem, S., Abbas, N., Saleem, A., Issakhov, A., 2020. Influence of Lorentz force and induced magnetic field effects on Casson micropolar nanofluid flow over a permeable curved stretching/shrinking surface under the stagnation region. Surf. Interfaces 21, 100766.

Besthapu, P., Haq, R.U., Bandari, S., Al-Mdallal, Q.M., 2017. Mixed convection flow of thermally stratified MHD nanofluid over an exponentially stretching surface with viscous dissipation effect. J. Taiwan Inst. Chem. Eng. 71, 307–314.

Buongiorno, J., Venerus, D.C., Prabhat, N., McKrell, T., Townsend, J., Christianson, R., Zhou, S.Q., 2009. A benchmark study on the thermal conductivity of nanofluids. J. Appl. Phys. 106 (9).

Chen, C.H., 2007. Marangoni effects on forced convection of power-law liquids in a thin film over a stretching surface. Phys. Lett. A 370 (1), 51–57.

Choi, S.U., Eastman, J.A., 1995 Oct 1. Enhancing Thermal Conductivity of Fluids With Nanoparticles. Argonne National Lab.(ANL), Argonne, IL (United States).

Das, K., Acharya, N., Kundu, P.K., 2016. The onset of nanofluid flow past a convectively heated shrinking sheet in presence of heat source/sink: a Lie group approach. Appl. Therm. Eng. 103, 38–46.

Eastman, J.A., Choi, U.S., Li, S., Thompson, L.J., Lee, S., 1996. Enhanced thermal conductivity through the development of nanofluids. MRS Online Proc. Library (OPL) 457, 3.

Ellahi, R., Zeeshan, A., Hassan, M., 2016. Particle shape effects on Marangoni convection boundary layer flow of a nanofluid. Int. J. Numer. Methods Heat Fluid Flow 26 (7), 2160–2174.

Gul, T., Bilal, M., Saeed, A., Alghamdi, W., Mukhtar, S., Alrabaiah, H., Bonyah, E., 2020a. Viscous dissipated hybrid nanoliquid flow with Darcy–Forchheimer and forced convection over a moving thin needle. AIP Adv. 10 (10).

Gul, T., Rahman, J.U., Bilal, M., Saeed, A., Alghamdi, W., Mukhtar, S., Bonyah, E., 2020b. Viscous dissipated hybrid nanoliquid flow with Darcy–Forchheimer and forced convection over a moving thin needle. AIP Adv. 10 (10), 105308.

Hameed, N., Noeiaghdam, S., Khan, W., Pimpunchat, B., Fernandez-Gamiz, U., Khan, M. S., Rehman, A., 2022. Analytical analysis of the magnetic field, heat generation and absorption, viscous dissipation on couple stress casson hybrid nano fluid over a nonlinear stretching surface. Results Eng. 16, 100601.

Ishfaq, N., Khan, Z.H., Khan, W.A., Culham, R.J., 2016. Estimation of boundary-layer flow of a nanofluid past a stretching sheet: a revised model. J. Hydrodyn. 28 (4), 596–602.

Javed, M., Imran, N., Arooj, A., Sohail, M., 2021. Meta-analysis on homogeneous-heterogeneous reaction effects in a sinusoidal wavy curved channel. Chem. Phys. Lett. 763, 138200.

Jiao, C., Zheng, L., Lin, Y., Ma, L., Chen, G., 2016. Marangoni abnormal convection heat transfer of power-law fluid driven by temperature gradient in porous medium with heat generation. Int. J. Heat Mass Transf. 92, 700–707.

Kandasamy, R., Mohamad, R., Ismoen, M., 2016. Impact of chemical reaction on Cu, Al2O3 and SWCNTs–nanofluid flow under slip conditions. Eng. Sci. Technol. Int. J. 19 (2), 700–709.

Khan, D., Kumam, P., Khan, I., Khan, A., Watthayu, W., Arif, M., 2022. Scientific investigation of a fractional model based on hybrid nanofluids with heat generation and porous medium: applications in the drilling process. Sci. Rep. 12 (1), 6524.

Khan, D., Kumam, P., Watthayu, W., Yassen, M.F., 2023. A novel multi fractional comparative analysis of second law analysis of MHD flow of Casson nanofluid in a porous medium with slipping and ramped wall heating. ZAMM-J. Appl. Math. Mech./Z. Angew. Math. Mech., e202100424

Khan, W.A., Pop, I., 2010. Boundary-layer flow of a nanofluid past a stretching sheet. Int. J. Heat Mass Transf. 53 (11–12), 2477–2483.

Lin, Y., Zheng, L., Zhang, X., 2013. Magnetohydrodynamics thermocapillary Marangoni convection heat transfer of power-law fluids driven by temperature gradient. J. Heat Transf. 135 (5), 051702.

Lin, Y., Zheng, L., Zhang, X., 2014. Radiation effects on Marangoni convection flow and heat transfer in pseudo-plastic non-Newtonian nanofluids with variable thermal conductivity. Int. J. Heat Mass Transf. 77, 708–716.

Magyari, E., Chamkha, A.J., 2007. Exact analytical solutions for thermosolutal Marangoni convection in the presence of heat and mass generation or consumption. Heat Mass Transf. 43 (9), 965–974.

Makinde, O.D., Aziz, A., 2011. Boundary layer flow of a nanofluid past a stretching sheet with a convective boundary condition. Int. J. Therm. Sci. 50 (7), 1326–1332.

Makinde, O.D., Mabood, F., Khan, W.A., Tshehla, M.S., 2016. MHD flow of a variable viscosity nanofluid over a radially stretching convective surface with radiative heat. J. Mol. Liq. 219, 624–630.

Merkin, J.H., 1986. On dual solutions occurring in mixed convection in a porous medium. J. Eng. Math. 20 (2), 171–179.

Mohyud-Din, S.T., Khan, U., Ahmed, N., Sikander, W., 2015. A study of velocity and temperature slip effects on flow of water based nanofluids in converging and diverging channels. Int. J. Appl. Comput. Math. 1 (4), 569–587.

Moldoveanu, G.M., Minea, A.A., Huminic, G., Huminic, A., 2019. Al 2 O 3/TiO 2 hybrid nanofluids thermal conductivity: an experimental approach. J. Therm. Anal. Calorim. 137, 583–592.

Nadeem, S., Khan, M.N., Abbas, N., 2020. Transportation of slip effects on nanomaterial micropolar fluid flow over exponentially stretching. Alex. Eng. J. 59 (5), 3443–3450.

Naseem, T., Nazir, U., Sohail, M., 2021. Contribution of Dufour and Soret effects on hydromagnetized material comprising temperature-dependent thermal conductivity. Heat Transf. 50 (7), 7157–7175.

Nazir, U., Sohail, M., Mukdasai, K., Singh, A., Alahmadi, R.A., Galal, A.M., Eldin, S.M., 2022. Applications of variable thermal properties in Carreau material with ion slip and Hall forces towards cone using a non-Fourier approach via FE-method and mesh-free study. Front. Mater. 9, 1054138.

Nazir, U., Sohail, M., Selim, M.M., Alrabaiah, H., Kumam, P., 2021. Finite element simulations of hybrid nano-Carreau Yasuda fluid with hall and ion slip forces over rotating heated porous cone. Sci. Rep. 11 (1), 19604.

Pop, I., Postelnicu, A., Groşan, T., 2001. Thermosolutal Marangoni forced convection boundary layers. Meccanica 36 (5), 555–571.

Rana, P., Bhargava, R., 2012. Flow and heat transfer of a nanofluid over a nonlinearly stretching sheet: a numerical study. Commun. Nonlinear Sci. Numer. Simul. 17 (1), 212–226.

Rana, P., Bhargava, R., Bég, O.A., 2012. Numerical solution for mixed convection boundary layer flow of a nanofluid along an inclined plate embedded in a porous medium. Comput. Math. Appl. 64 (9), 2816–2832.

Rehman, A., Khan, W., Bonyah, E., Abdul Karim, S.A., Alshehri, A., Galal, A.M, 2022a. Steady three-dimensional MHD mixed convection couple stress flow of hybrid nanofluid with hall and ion slip effect. Adv. Civil Eng. 2022.

Rehman, A., Saeed, A., Salleh, Z., Jan, R., Kumam, P., 2022b. Analytical investigation of the time-dependent stagnation point flow of a CNT nanofluid over a stretching surface. Nanomaterials 12 (7), 1108.

Rehman, A., Salleh, Z., 2021. Analytical investigation of magnetic field on unsteady boundary layer stagnation point flow of water-based graphene oxide-water and graphene oxide-ethylene glycol nanofluid over a stretching surface. Math. Probl. Eng. 2021.

Rizk, D., Ullah, A., Elattar, S., Alharbi, K.A.M., Sohail, M., Khan, R., Mlaiki, N., 2022. Impact of the KKL correlation model on the activation of thermal energy for the hybrid nanofluid (GO+ ZnO+ Water) flow through permeable vertically rotating surface. Energies 15 (8), 2872.

Shatanawi, W., Abbas, N., Shatnawi, T.A., Hasan, F., 2023. Heat and mass transfer of generalized fourier and Fick's law for second-grade fluid flow at slendering vertical Riga sheet. Heliyon 9 (3).

Sheikholeslami, M., Chamkha, A.J., 2017. Influence of Lorentz forces on nanofluid forced convection considering Marangoni convection. J. Mol. Liq. 225, 750–757.

Sohail, M., Ali, U., Al-Mdallal, Q., Thounthong, P., Sherif, E.S.M., Alrabaiah, H., Abdelmalek, Z., 2020a. Theoretical and numerical investigation of entropy for the variable thermophysical characteristics of couple stress material: applications to optimization. Alex. Eng. J. 59 (6), 4365–4375.

Sohail, M., Chu, Y.M., El-Zahar, E.R., Nazir, U., Naseem, T., 2021. Contribution of joule heating and viscous dissipation on three dimensional flow of Casson model comprising temperature dependent conductance utilizing shooting method. Phys. Scr. 96 (8), 085208.

Sohail, M., Nazir, U., Chu, Y.M., Alrabaiah, H., Al-Kouz, W., Thounthong, P., 2020b. Computational exploration for radiative flow of Sutterby nanofluid with variable temperature-dependent thermal conductivity and diffusion coefficient. Open Phys. 18 (1), 1073–1083.

Wakif, A., Chamkha, A., Thumma, T., Animasaun, I.L., Sehaqui, R., 2021. Thermal radiation and surface roughness effects on the thermo-magneto-hydrodynamic stability of alumina–copper oxide hybrid nanofluids utilizing the generalized Buongiorno's nanofluid model. J. Therm. Anal. Calorim. 143, 1201–1220.
Wang, C.Y., 1991. Fluid film sprayed on a stretching surface. Chem. Eng. Commun. 107 (1), 11–19.
Wang, F., Nazir, U., Sohail, M., El-Zahar, E.R., Park, C., Thounthong, P., 2022. A Galerkin strategy for tri-hybridized mixture in ethylene glycol comprising variable diffusion and thermal conductivity using non-Fourier's theory. Nanotechnol. Rev. 11 (1), 834–845.
Weidman, P.D., Kubitschek, D.G., Davis, A.M.J., 2006. The effect of transpiration on self-similar boundary layer flow over moving surfaces. Int. J. Eng. Sci. 44 (11–12), 730–737.
Zubair, T., Usman, M., Hamid, M., Sohail, M., Nazir, U., Nisar, K.S., Vijayakumar, V., 2021. Computational analysis of radiative Williamson hybrid nanofluid comprising variable thermal conductivity. Jpn. J. Appl. Phys. 60 (8), 087004.